Analysis and numerical simulation of an induction–conduction model arising in steel heat treating

J.M. Díaz Moreno [a], C. García Vázquez [a], M.T. González Montesinos [b], F. Ortegón Gallego [a]

[a] *Departamento de Matemáticas, Universidad de Cádiz, 11510 Puerto Real, Cádiz, Spain*
[b] *Departamento de Matemática Aplicada I, Universidad de Sevilla, Avda. de Reina Mercedes, s/n, 41012 Sevilla, Spain*

Keywords:
Steel hardening
Phase fractions
Nonlinear parabolic–elliptic equations
Sobolev spaces
Finite elements method

A B S T R A C T

The goal of steel heat treating is to create a hard enough part over certain critical surfaces or volumes of the workpiece and at the same time keeping its ductility properties all over the rest of the workpiece.

We consider a mathematical model for the description of the heating–cooling industrial process of a steel workpiece. This model consists of a nonlinear coupled partial differential system of equations involving the electric potential, the magnetic vector potential, the temperature, together with a system of ordinary differential equations for the steel phase fractions. Due to the different time scales related to the electric potential and the magnetic vector potential versus the temperature, we introduce the harmonic regime, leading to a new system of nonlinear PDEs. Finally, we have carried out some 2D numerical simulations of this heating–cooling industrial process.

1. Introduction

This work deals with the mathematical analysis and numerical simulations of a model governed in terms of a nonlinear system of partial differential equations/ordinary differential equations describing the industrial process of steel hardening, including phase transitions. This subject has been extensively studied during the last few years [1–5]. A complete model, including thermomechanical effects can be seen, for instance, in [5]. Here our main concern is the description of the temperature, dropping out mechanical effects. The mathematical model is governed by a coupled nonlinear system of PDEs/ODEs, namely

$$\left.\begin{array}{l}
\nabla\cdot(\sigma(\theta)\nabla\phi)=0 \quad \text{in } \Omega_T=\Omega\times(0,T),\\
\sigma_0(\theta)\boldsymbol{\mathcal{A}}_t+\nabla\times\left(\dfrac{1}{\mu}\nabla\times\boldsymbol{\mathcal{A}}\right)-\delta\nabla(\nabla\cdot\boldsymbol{\mathcal{A}})=-\sigma_0(\theta)\nabla\phi \quad \text{in } D_T=D\times(0,T),\\
\boldsymbol{\mathcal{A}}(0)=\boldsymbol{\mathcal{A}}_0 \quad \text{in } \Omega,\\
z_t=F(\theta,z) \quad \text{in } \Omega_T^s=\Omega^s\times(0,T),\\
z(0)=z_0 \quad \text{in } \Omega^s,\\
\rho c_\epsilon\theta_t-\nabla\cdot(\kappa(\theta)\nabla\theta)=\sigma_0(\theta)|\boldsymbol{\mathcal{A}}_t+\nabla\phi|^2+\rho L z_t+G \quad \text{in } \Omega_T,\\
\theta(0)=\theta_0 \quad \text{in } \Omega.
\end{array}\right\} \tag{1}$$

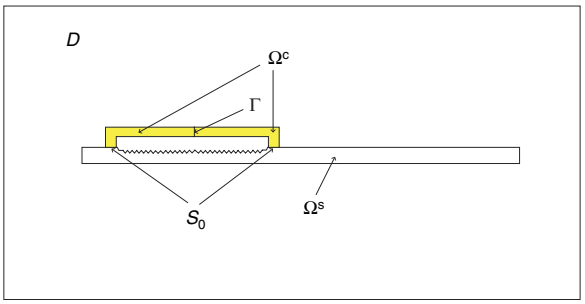

Fig. 1. Domains D, $\Omega = \Omega^s \cup \Omega^c \cup S_0$ and the interface $\Gamma \subset \Omega^c$. The inductor Ω^c is made of copper. The workpiece contains a toothed part to be hardened by means of the heating–cooling process described below. It is made of a hypoeutectoid steel.

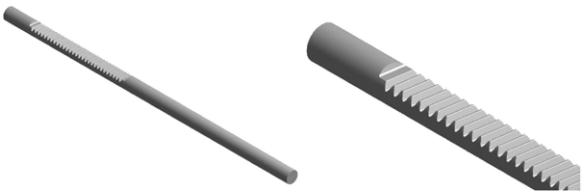

Fig. 2. Car steering rack.

where $\Omega, D \subset \mathbb{R}^N$, $N = 2$ or 3, are bounded, connected and Lipschitz-continuous open sets such that $\bar{\Omega} \subset D$, $\Omega = \Omega^c \cup \Omega^s \cup S$ is the set of conductors, Ω^c the inductor (usually made of copper), Ω^s the steel workpiece, Ω^c and Ω^s being open sets, and $S = \bar{\Omega}^c \cap \bar{\Omega}^s$ is the surface contact between Ω^c and Ω^s, $\Omega^c \cap \Omega^s = \varnothing$ (see Fig. 1); T stands for the final time of observation; ϕ the electrical potential; $\mathcal{A}$ the magnetic vector potential; G a given external source coming for the mechanical deformation (here assumed to be known); θ the temperature; $z = (z_1, z_2)$, z_1 and z_2 are the phase fractions [6,7,3] of austenite and martensite, respectively; $F = (F_1, F_2)$ gives the phase fractions model; $\kappa(\theta)$ is the thermal conductivity; $\sigma(\theta)$ the electrical conductivity (by $\sigma(\theta)$ we mean the function $(x, t) \mapsto \sigma(x, \theta(x, t))$, and also for $\kappa(\theta)$, etc.); $\sigma_0(x, s) = \sigma(x, s)$ if $x \in \bar{\Omega}$, $\sigma_0(x, s) = 0$ elsewhere; $\mu = \mu(x)$ is the magnetic permeability; ρ the density; $L = (L_1, L_2)$ is the latent heat; c_ϵ is the specific heat capacity at constant strain; $\delta > 0$ is a small constant. System (1) is supplied with suitable boundary conditions.

The induction–conduction model (1) describes the heating process of a steel workpiece. Once the desired high level of temperature is reached at certain critical parts along the workpiece, the supplied electric current is switched off and the workpiece is then quenched in order to cool it down rapidly. The goal is to produce martensite (hard and brittle steel phase transition) in these critical parts, keeping the rest ductile. Usually, these parts correspond to particular structural components whose surface is going to be highly stressed during its mechanical lifetime. This is the case of a car steering rack (see Fig. 2).

In [5], it is assumed the Coulomb gage condition for the magnetic vector potential, namely, $\nabla \cdot \mathcal{A} = 0$. In our analysis, we do not impose this condition since this makes an undesired pressure gradient appear in the equation for $\mathcal{A}$. In its turn, we include a penalty term in this equation of the form $-\delta \nabla(\nabla \cdot \mathcal{A})$.

2. The mathematical description for the heating–cooling process

We split the time interval $[0, T]$ into two intervals: $[0, T] = [0, T_h) \cup [T_h, T_c]$, $T_c > T_h > 0$. The first one $[0, T_h)$ corresponds to the heating process. All along this time interval, a high frequency electric current is supplied through the conductor which in its turn induces a magnetic field. The combined effect of both conduction and induction gives rise to a production term in the energy balance equation, namely $b(\theta)|\mathcal{A}_t + \nabla\phi|^2$. This is Joule's heating. At the instant $t = T_h$, the current is switched off and during the time interval $[T_h, T_c]$ the workpiece is cooled down by means of aqua-quenching.

2.1. The heating model

The current passing through the set of conductors $\Omega = \Omega^c \cup \Omega^s$ is modeled with the aid of an auxiliary smooth surface $\Gamma \subset \Omega^c$ cutting the inductor Ω^c into two parts, each one of them having a surface contact over the boundary of the workpiece Ω^s (see Fig. 1). For the sake of simplicity, we will assume that $\rho c_\epsilon = 1$. The heating model reads as follows

$$\nabla \cdot (\sigma(\theta)\nabla\phi) = 0 \quad \text{in } \Omega_{T_h} = \Omega \times (0, T_h), \tag{2}$$

$$\frac{\partial \phi}{\partial n} = 0 \quad \text{on } \partial\Omega \times (0, T_h), \tag{3}$$

$$\left[\sigma(\theta)\frac{\partial\phi}{\partial n}\right]_{\Gamma} = j_S \quad \text{on } \Gamma \times (0, T_{\mathrm{h}}), \tag{4}$$

$$\sigma_0(\theta)\boldsymbol{\mathcal{A}}_t + \nabla \times \left(\frac{1}{\mu}\nabla \times \boldsymbol{\mathcal{A}}\right) - \delta\nabla(\nabla \cdot \boldsymbol{\mathcal{A}}) = -\sigma_0(\theta)\nabla\phi \quad \text{in } D \times (0, T_{\mathrm{h}}), \tag{5}$$

$$\boldsymbol{\mathcal{A}} = 0 \quad \text{on } \partial D \times (0, T_{\mathrm{h}}), \tag{6}$$

$$\boldsymbol{\mathcal{A}}(0) = \boldsymbol{\mathcal{A}}_0 \quad \text{in } \Omega, \tag{7}$$

$$z_t = F(\theta, z) \quad \text{in } \Omega^{\mathrm{s}} \times (0, T_{\mathrm{h}}), \tag{8}$$

$$z(0) = z_0 \quad \text{in } \Omega^{\mathrm{s}}, \tag{9}$$

$$\theta_t - \nabla \cdot (\kappa(\theta)\nabla\theta) = \sigma_0(\theta)|\boldsymbol{\mathcal{A}}_t + \nabla\phi|^2 + \rho L z_t + G \quad \text{in } \Omega_{T_{\mathrm{h}}}, \tag{10}$$

$$\frac{\partial\theta}{\partial n} = 0 \quad \text{on } \partial\Omega \times (0, T_{\mathrm{h}}), \tag{11}$$

$$\theta(0) = \theta_0 \quad \text{in } \Omega. \tag{12}$$

In (4) $[\,\cdot\,]_{\Gamma}$ stands for the jump across the inner surface Γ. The function j_S represents the external source current density. The domain D containing the set of conductors is taken big enough so that the magnetic vector potential $\boldsymbol{\mathcal{A}}$ vanishes on its boundary ∂D. Since z is only defined in Ω^{s}, the term $\rho L z_t$ appearing in (10), and in (15) below, is assumed to be zero outside Ω^{s}.

2.2. The cooling model

Once the heating process ends, aqua-quenching begins. This situation is modeled via the Robin boundary condition given in (16).

We put $z_{T_{\mathrm{h}}} = z(T_{\mathrm{h}})$, that is, $z_{T_{\mathrm{h}}}$ is the phase fraction distribution at the final heating instant T_{h} obtained from (8). In the same way, we define $\theta_{T_{\mathrm{h}}} = \theta(T_{\mathrm{h}})$. Obviously, these functions will be taken as the initial phase fraction distribution and temperature, respectively, in the cooling model.

$$z_t = F(\theta, z) \quad \text{in } \Omega^{s} \times (T_{\mathrm{h}}, T_{\mathrm{c}}), \tag{13}$$

$$z(T_{\mathrm{h}}) = z_{T_{\mathrm{h}}} \quad \text{in } \Omega^{s}, \tag{14}$$

$$\theta_t - \nabla \cdot (\kappa(\theta)\nabla\theta) = \rho L z_t + G \quad \text{in } \Omega \times (T_{\mathrm{h}}, T_{\mathrm{c}}), \tag{15}$$

$$-\kappa(\theta)\frac{\partial\theta}{\partial n} = \beta(\theta - \theta_{\mathrm{e}}) \quad \text{on } \partial\Omega \times (T_{\mathrm{h}}, T_{\mathrm{c}}), \tag{16}$$

$$\theta(T_{\mathrm{h}}) = \theta_{T_{\mathrm{h}}} \quad \text{in } \Omega. \tag{17}$$

In (16), the constant value θ_{e} stands for the temperature of the spray water quenching the workpiece during the cooling time interval $[T_{\mathrm{h}}, T_{\mathrm{c}}]$. Also, the function β is a heat transfer coefficient and is given by

$$\beta(x, t) = \begin{cases} 0 & \text{on } \partial\Omega \cap \partial\Omega^{\mathrm{c}}, \\ \beta_0(t) & \text{on } \partial\Omega \cap \partial\Omega^{\mathrm{s}}, \end{cases}$$

where $\beta_0(t) > 0$ (usually taken to be constant).

3. The harmonic regime

We focus our attention on the heating induction–conduction process. For this reason and from now on, we will just write T instead of T_{h}.

Electromagnetic fields generated by high frequency currents are sinusoidal in time. Consequently, both the electric potential, ϕ, and the magnetic vector potential, $\boldsymbol{\mathcal{A}}$, take the form [6–9] $\mathcal{M}(x, t) = \mathrm{Re}[\exp(\mathrm{i}\omega t)M(x)]$, where M is a complex-valued function or vector field, and $\omega = 2\pi f$ is the angular frequency, f being the electric current frequency. In general, M also depends on t, but at a time scale much greater than $1/\omega$. In this way, we may introduce the complex-valued fields φ, $\boldsymbol{A}$ and $\boldsymbol{j}$ as

$$\phi = \mathrm{Re}[\exp(\mathrm{i}\omega t)\varphi(x, t)], \qquad \boldsymbol{\mathcal{A}} = \mathrm{Re}[\exp(\mathrm{i}\omega t)\boldsymbol{A}(x, t)], \qquad j_S = \mathrm{Re}[\exp(\mathrm{i}\omega t)\boldsymbol{j}(x, t)].$$

As a far as the numerical simulation of a system like (2)–(12) is concerned, the introduction of the new variables φ and $\boldsymbol{A}$ is quite convenient since the time scale describing the evolution of both φ and $\boldsymbol{A}$ is much smaller than that of the temperature θ. In the case of steel heat treating, f is about 80 kHz.

When we rewrite the original system (2)–(12) in terms of the new complex-valued variables, φ and $\boldsymbol{A}$, neglecting the term $\boldsymbol{A}_t$, we obtain the so-called harmonic regime. Furthermore, in the energy equation, the expression $|\mathscr{A}_t + \nabla\phi|^2$ is substituted by its mean value measured over a time period $[t, t+\omega]$:

$$\frac{1}{\omega}\int_t^{t+\omega} |\mathscr{A}_t + \nabla\phi|^2 \simeq \frac{1}{2}|\mathrm{i}\omega\boldsymbol{A} + \nabla\varphi|^2.$$

In this way, the effective Joule's heating takes the form $\frac{1}{2}\sigma(\theta)|\mathrm{i}\omega\boldsymbol{A} + \nabla\varphi|^2$. The equations in the harmonic regime are the following.

$$\nabla\cdot(\sigma(\theta)\nabla\varphi) = 0 \quad \text{in } \Omega_T, \tag{18}$$

$$\frac{\partial\varphi}{\partial n} = 0 \quad \text{on } \partial\Omega\times(0,T), \tag{19}$$

$$\left[\sigma(\theta)\frac{\partial\varphi}{\partial\nu}\right]_\Gamma = \boldsymbol{j} \quad \text{on } \Gamma\times(0,T), \tag{20}$$

$$\mathrm{i}\omega\sigma_0(\theta)\boldsymbol{A} + \nabla\times\left(\frac{1}{\mu}\nabla\times\boldsymbol{A}\right) - \delta\nabla(\nabla\cdot\boldsymbol{A}) = -\sigma_0(\theta)\nabla\varphi \quad \text{in } D_T, \tag{21}$$

$$\boldsymbol{A} = 0 \quad \text{on } \partial D\times(0,T), \tag{22}$$

$$z_t = F(\theta, z) \quad \text{in } \Omega^s\times(0,T), \tag{23}$$

$$z(0) = z_0 \quad \text{in } \Omega^s, \tag{24}$$

$$\theta_t - \nabla\cdot(\kappa(\theta)\nabla\theta) = \frac{1}{2}\sigma(\theta)|\mathrm{i}\omega\boldsymbol{A} + \nabla\varphi|^2 + \rho L z_t + G \quad \text{in } \Omega_T, \tag{25}$$

$$\frac{\partial\theta}{\partial n} = 0 \quad \text{on } \partial\Omega\times(0,T), \tag{26}$$

$$\theta(\cdot,0) = \theta_0 \quad \text{in } \Omega. \tag{27}$$

Remark. A similar simpler stationary model involving only the unknowns φ, $\boldsymbol{A}$ and θ and with non-homogeneous Dirichlet boundary conditions is studied in [10].

4. An existence result

We consider the system (18)–(27) describing the heating process by conduction–induction in the harmonic regime. Besides the assumptions on data already mentioned along the introduction, we will consider the following hypotheses.

(H.1) $\sigma, \kappa : \Omega\times\mathbb{R} \mapsto \mathbb{R}$ are Carathéodory functions and there exist some constant values $\sigma_1, \sigma_2, \kappa_1, \kappa_2 \in \mathbb{R}$ such that $0 < \sigma_1 \le \sigma(x,s) \le \sigma_2$, $0 < \kappa_1 \le \kappa(x,s) \le \kappa_2$, almost everywhere $x \in \Omega$ and for all $s \in \mathbb{R}$.
(H.2) $\boldsymbol{j} \in L^2(0,T; H^{-1/2}(\Gamma))$ and $\langle \boldsymbol{j}(t), 1\rangle_\Gamma = 0$, almost everywhere $t \in (0, T_h)$.
Here, $\langle\cdot,\cdot\rangle_\Gamma$ stands for the duality pair between $H^{-1/2}(\Gamma)$ and $H^{1/2}(\Gamma)$.
(H.3) $\mu \in L^\infty(D)$ and there exists a constant value μ_* such that $0 < \mu_* \le \mu$ in D.
(H.4) $F \in L^\infty(\mathbb{R}\times\mathbb{R}^2) \cap C(\mathbb{R}\times\mathbb{R}^2)$ and there exists a constant L_F such that $|F(s,s_1) - F(s,s_2)| \le L_F|s_1 - s_2|$, for all $s \in \mathbb{R}$ and for all $s_1, s_2 \in \mathbb{R}^2$.
(H.5) $z_0 = (z_{01}, z_{02}) \in L^\infty(\Omega^s)$.
(H.6) $\rho L, G \in L^1(\Omega^s\times(0,T))$.
(H.7) $\theta_0 \in L^1(\Omega)$.

Remark. In the situation described here, we are just considering the evolution of two phase fractions which correspond to austenite and martensite. Of course, we may consider a more general setting which includes other phase fractions like bainite, pearlite and ferrite or a mix of them all (see [4]).

Remark. In practice, the magnetic permeability is of the form

$$\mu(x) = \mu_1\chi_{\Omega^s} + \mu_2\chi_{\Omega^c} + \mu_3\chi_{D\setminus\Omega},$$

where $\mu_i > 0$, $1 \le i \le 3$, are constant values such that $\mu_2 < \mu_3 \ll \mu_1$.

4.1. Variational formulation

The variational formulation corresponding to the system (18)–(27) allows us to give the concept of a solution $(\varphi, \boldsymbol{A}, z, \theta)$ to this system.

We denote by $H^1(\Omega) = \{v \in L^2(\Omega) / \nabla v \in (L^2(\Omega))^N\}$, $N = 2$ or 3, the complex-valued usual Sobolev space, the derivatives of v taken in the sense of distributions. We also use the complex-valued Sobolev space $H_0^1(D) = \{v \in H^1(D) / v = 0 \text{ on } \partial D\}$. Then we put $\boldsymbol{H}_0^1(D) = (H_0^1(D))^N$. All these spaces are Hilbert spaces provided with their respective inner products.

The quotient space $H^1(\Omega)/\mathbb{C}$ is a Hilbert space provided with the inner product $(\dot{u}, \dot{v}) = \int_\Omega \nabla u \nabla \bar{v}$, where u, respectively v, is any element in the class of $\dot{u}$, respectively $\dot{v}$, and $\bar{v}$ stands for the conjugate of v.

For $1 \le p \le \infty$, we also consider the Banach (real) space $W^{1,p}(\Omega)$ provided with their standard norm, and $(W^{1,p}(\Omega))'$ its dual (topological and algebraic) space.

If X is a Banach space, we put $L^p(X) = L^p(0, T; X)$ and $W^{1,p}(X) = W^{1,p}(0, T; X)$, that is $W^{1,p}(X) = \{v \in L^p(X) / v_t \in L^p(X)\}$, the derivative v_t taken in the sense of distributions in $(0, T)$. Both, $L^p(X)$ and $W^{1,p}(X)$ are Banach spaces. Remember that $W^{1,p}(X) \subset C([0, T]; X)$ with continuous embedding.

Definition 1. We say that $(\varphi, \boldsymbol{A}, z, \theta)$ is a weak solution to the system (18)–(27) if the following conditions hold

$$\varphi \in L^2(H^1(\Omega)/\mathbb{C}), \tag{28}$$

$$\boldsymbol{A} \in L^2(\boldsymbol{H}_0^1(D)), \tag{29}$$

$$z \in W^{1,\infty}(L^\infty(\Omega^s)), \tag{30}$$

$$\theta \in L^p(W^{1,p}(\Omega)) \cap C([0, T]; (W^{1,p'}(\Omega))') \quad \text{for all } p \in \left[1, \frac{N+2}{N+1}\right), \ \frac{1}{p} + \frac{1}{p'} = 1, \tag{31}$$

$$\theta(\cdot, 0) = \theta_0 \quad \text{in } \Omega, \tag{32}$$

$$\int_0^T \int_\Omega \sigma(\theta) \nabla\varphi \cdot \nabla\bar{\psi} + \int_0^T \langle \boldsymbol{j}, \bar{\psi} \rangle_\Gamma = 0, \quad \text{for all } \psi \in L^2(H^1(\Omega)/\mathbb{C}), \tag{33}$$

$$\begin{aligned} &\mathrm{i}\omega \int_0^T \int_\Omega \sigma(\theta) \boldsymbol{A} \cdot \bar{\boldsymbol{\nu}} + \int_0^T \int_D \frac{1}{\mu} \nabla \times \boldsymbol{A} \cdot \nabla \times \bar{\boldsymbol{\nu}} + \delta \int_0^T \int_D \nabla \cdot \boldsymbol{A} \nabla \cdot \bar{\boldsymbol{\nu}} + \int_0^T \int_\Omega \sigma(\theta) \nabla\varphi \cdot \bar{\boldsymbol{\nu}} = 0, \\ &\quad \text{for all } \boldsymbol{\nu} \in L^2(\boldsymbol{H}_0^1(D)) \end{aligned} \tag{34}$$

$$z = z_0 + \int_0^t F(\theta, z), \quad \text{for all } t \in [0, T] \tag{35}$$

$$\begin{aligned} &-\int_0^T \int_\Omega \theta \zeta_t + \int_0^T \int_\Omega \kappa(\theta) \nabla\theta \nabla\zeta = \int_0^T \int_\Omega \left(\frac{1}{2}\sigma(\theta)|\mathrm{i}\omega\boldsymbol{A} + \nabla\varphi|^2 + \rho L z_t + G\right)\zeta, \\ &\quad \text{for all } \zeta \in \mathcal{C}^1(\bar{\Omega} \times [0, T]) \text{ such that } \zeta(\cdot, 0) = \zeta(\cdot, T) = 0 \text{ in } \Omega. \end{aligned} \tag{36}$$

Remark. As long as $N \le 3$, Sobolev embedding implies that $L^1(\Omega) \subset (W^{1,q}(\Omega))'$ for all $q > 3$. On the other hand, since $p < 5/4 \le (N+2)/(N+1)$ we have $p' > 5$; in particular, $L^1(\Omega) \subset (W^{1,p'}(\Omega))'$ for all $p \in [1, 5/4)$. Consequently, according to (H.7) and the regularity $\theta \in C([0, T]; (W^{1,p'}(\Omega))')$ stated in (31), the initial condition (32) makes sense at least in the space $(W^{1,p'}(\Omega))'$. Under a more restrictive assumption on the thermal conductivity κ (see (H.8) below), it can be shown that $\theta \in C([0, T]; L^1(\Omega))$. Thus, the initial condition (32) also makes sense in $L^1(\Omega)$.

4.2. The main result

An existence result of a weak solution $(\varphi, \boldsymbol{A}, z, \theta)$ to the system (18)–(27) is given below. To this end, we also consider the following hypothesis on the thermal conductivity κ.

(H.8) There exist $\varepsilon_0 > 0$ and $L_0 > 0$ such that for all $\varepsilon \in (0, \varepsilon_0]$ one has

$$|\kappa(x, s_1) - \kappa(x, s_2)| \le L_0 |s_1 - s_2|,$$

almost everywhere $x \in \Omega$ and for all $s_1, s_2 \in \mathbb{R}$ such that $|s_1 - s_2| < \varepsilon$.

Theorem 1. *Assume the assumptions* (H.1)–(H.7). *Then there exists a weak solution to the system* (18)–(27) *in the sense of Definition 1.*

Moreover, if the thermal conductivity κ verifies the assumption (H.8), *then $\theta \in C([0, T]; L^1(\Omega))$ and it also satisfies the variational formulation*

$$\begin{aligned} &-\int_0^T \int_\Omega \theta \zeta_t + \int_\Omega \theta(x, T)\zeta(x, T) - \int_\Omega \theta_0(x)\zeta(x, 0) + \int_0^T \int_\Omega \kappa(\theta)\nabla\theta\nabla\zeta \\ &= \int_0^T \int_\Omega \left(\frac{1}{2}\sigma(\theta)|\mathrm{i}\omega\boldsymbol{A} + \nabla\varphi|^2 + \rho L z_t + G\right)\zeta, \quad \textit{for all } \zeta \in \mathcal{C}^1(\bar{\Omega} \times [0, T]). \end{aligned}$$

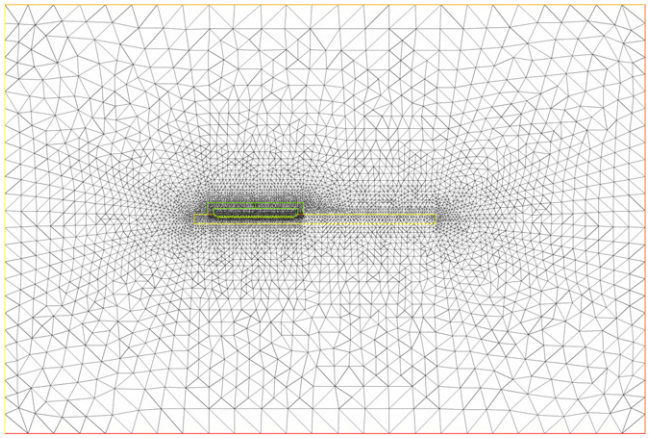

Fig. 3. Domain triangulation. This mesh of D contains 72,088 triangles and 36,095 vertices.

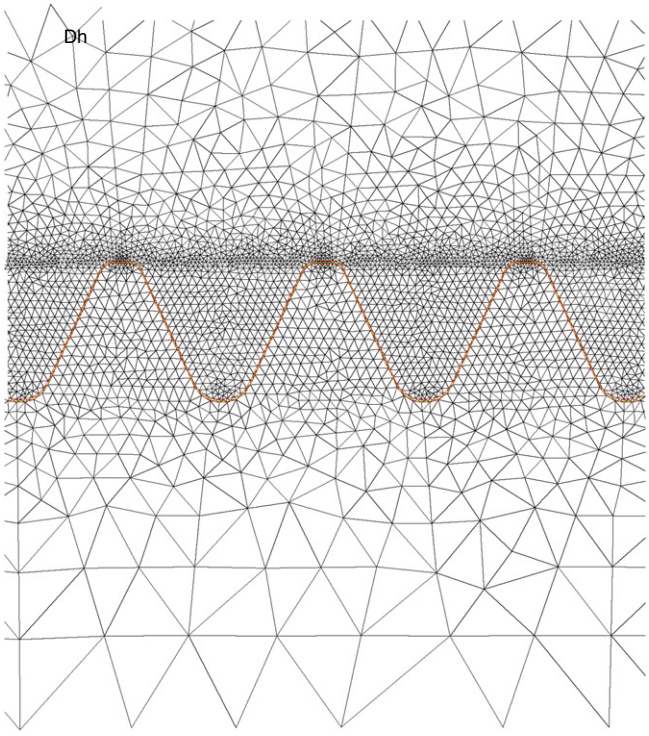

Fig. 4. Domain triangulation. Element density near three teeth.

The proof of this result will be developed in a forthcoming paper.

5. Numerical simulation

We have carried out some numerical simulations for the approximation of the solution to the system (18)–(27). We want to describe the hardening treatment of a car steering rack during the heating–cooling process. The goal is to produce martensite along the tooth line together with a thin layer in its neighborhood inside the steel workpiece.

Fig. 1 shows the open sets D, $\Omega = \Omega^s \cup \Omega^c \cup S$ and the interface Γ which intervene in the setting of the problem. The inductor Ω^c is made of copper. The workpiece contains a toothed part to be hardened by means of the heating–cooling process described above. It is made of a hypoeutectoid steel. The open set $D \setminus \bar{\Omega}$ is air. The magnetic permeability μ in (21)

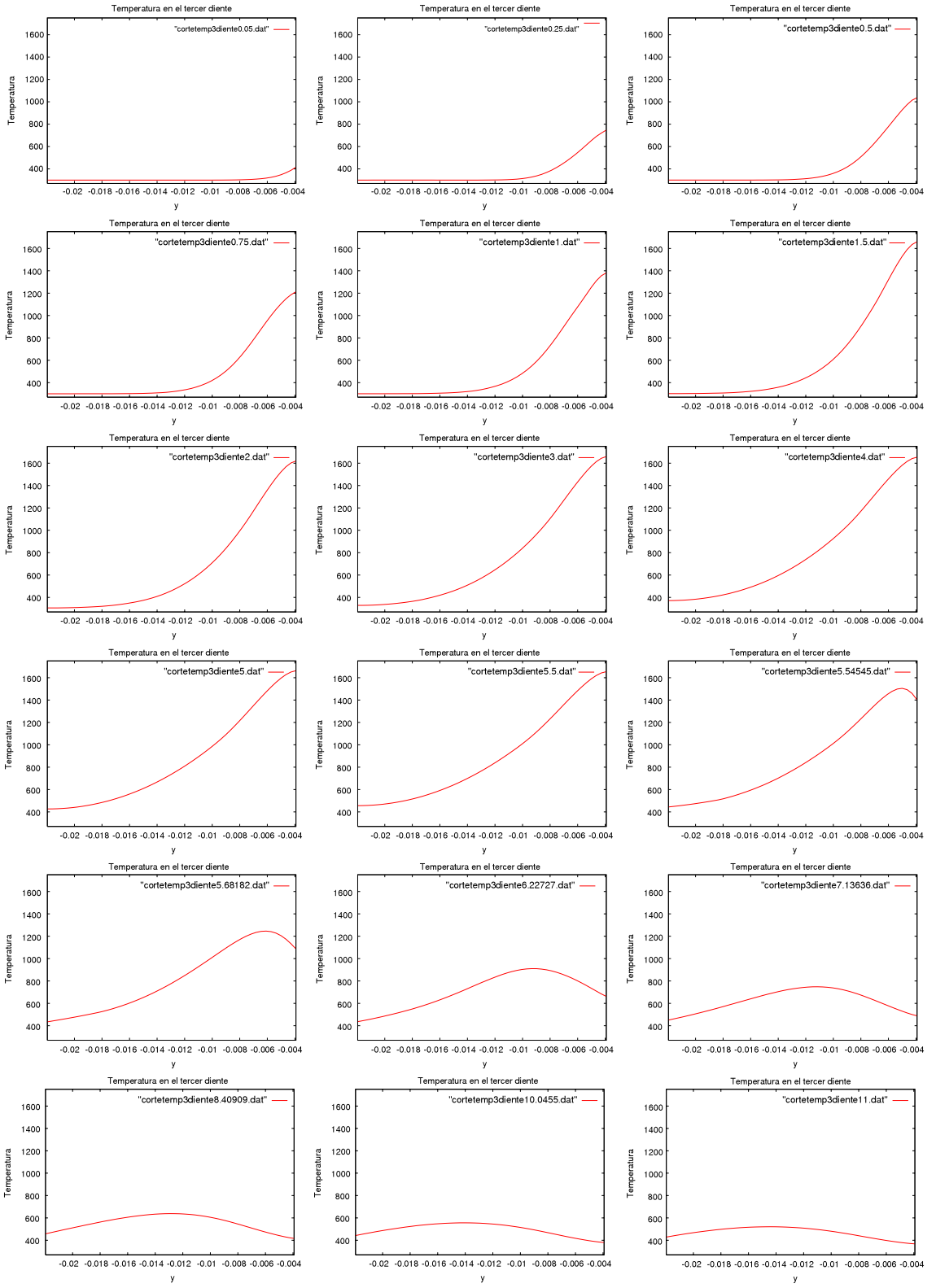

Fig. 5. Temperature profiles at $t = 0.05, 0.25, 0.5, 0.75, 1, 1.5, 2, 3, 4, 5, 5.5, 5.55, 5.68, 6.23, 7.14, 8.41, 10.05$ and 11 s, respectively, corresponding to a cut across the third tooth. The initial temperature in the rack is 300 K.

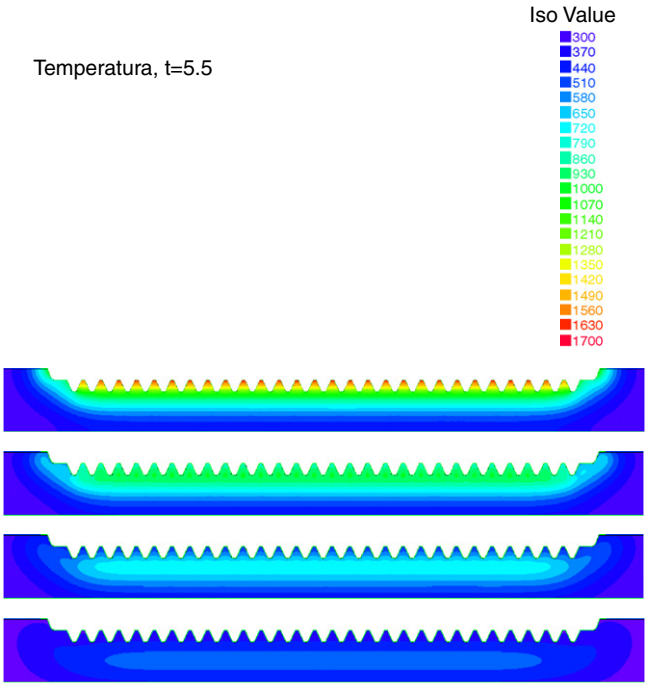

Fig. 6. Temperature distribution in the rack tooth line at time instants $t = 5.5$ (the heating stage ends), 5.97, 7.08 and 11 s, respectively.

is then given by

$$\mu(x) = \begin{cases} \mu_0 & \text{if } x \in D \setminus \bar{\Omega}, \\ 0.99995\mu_0 & \text{if } x \in \Omega^{\mathrm{c}}, \\ 2.24 \times 10^3 \mu_0 & \text{if } x \in \Omega^{\mathrm{s}}, \end{cases}$$

where $\mu_0 = 4\pi \times 10^{-7}$ (N/A^2) is the magnetic constant (vacuum permeability).

The martensite phase can only derive from the austenite phase. Thus we need to transform first the critical part to be hardened (the tooth line) into austenite. For our hypoeutectoid steel, austenite only exists in a temperature range close to the interval [1050, 1670] (in K). During the first stage, the workpiece is heated up by conduction and induction (Joule's heating) which renders the tooth line to the desired temperature. In order to transform the austenite into martensite, we must cool it down at a very high rate. This second stage is accomplished by spraying water over the workpiece. This latter process is called aqua-quenching.

In this simulation, the final time of the heating process is $T_{\mathrm{h}} = 5.5$ s and the cooling process extends also for 5.5 s, that is $T_{\mathrm{c}} = 11$.

We have used the finite elements method for the space approximation and a Crank–Nicolson scheme for the time discretization. Figs. 3 and 4 show the triangulation of D in our numerical simulations. We have used P_2-Lagrange approximation for φ, $\boldsymbol{A}$ and θ and P_1-Lagrange for z. All these numerical simulations have been carried out using the Freefem++ package [11]. Freefem++ is used as a pre-processor, in order to build up the mesh displayed in Figs. 3 and 4, as a solver to compute the discrete solutions, and as a post-processor, in order to visualize the numerical results.

In Fig. 6 we can see the temperature distribution in the rack along the tooth line at the final stage of the heating process and at three different time instants corresponding to the cooling process, including the final temperature distribution. The initial temperature is $\theta_0 = 300$ K. At $t = 5.5$ the heating process ends and the computed temperature shows that the temperature along the rack tooth line lies in the interval [1050, 1670] (K).

Fig. 5 shows different temperature profiles at the indicated time instants along a cross-section through the third tooth. The ordinate $y = -0.02$ corresponds to the upper boundary of the tooth. The first eleven pictures belong to the heating stage. We may observe the raising of the temperature at $y = -0.02$, due to the eddy currents and the skin effect. The interior of the tooth is then heated up by diffusion. At $t = 5.5$ the current is switched off and the aqua-quenching begins. The simulation shows how the workpiece is severely cooled down during the cooling stage.

Fig. 7 shows the austenization along the tooth line at the end of the heating process $T = 5.5$ s.

Fig. 8 shows the final distribution of martensite from austenite along the rack tooth line through the cooling stage $t = 11$ s. We have good agreement versus the experimental results obtained in the industrial process.

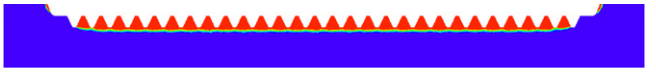

Fig. 7. Heating process. Austenite at $t = 5.5$ along the rack tooth line. Red is one and blue is zero. (For interpretation of the references to colour in this figure legend, the reader is referred to the web version of this article.)

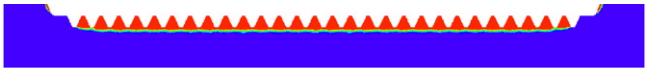

Fig. 8. Cooling process. Martensite transformation at the final stage of the cooling process $t = 11$ s. Red is one and blue is zero. (For interpretation of the references to colour in this figure legend, the reader is referred to the web version of this article.)

6. Conclusions

This paper describes a mathematical model for the industrial heating–cooling process of a steel workpiece corresponding to the steering rack of an automobile. Here, we are concerned with the description of the temperature in the workpiece so that mechanical effects are neglected in this analysis. In the industrial procedure, heating is produced by both induction and conduction through a high frequency current. We introduce Maxwell's equations in potential form which are strongly coupled with the temperature equation through temperature dependent diffusion coefficients and the so-called Joule's heating, the main responsible of bringing about heat in the steel workpiece along the critical surface to be hardened. For practical purposes, it is convenient to introduce the harmonic regime. We have performed some numerical simulations of the harmonic regime system for the heating stage, followed by the numerical simulation of the cooling process. The numerical results show reasonably well how the tooth line along the rack is heated up till austenization is reached. During aqua-quenching, the workpiece is severely cooled down at a high rate so that martensite is obtained where it is needed. As a result, the workpiece is hardened all along the tooth line, keeping the rest ductile.

In future works, we will take into account mechanical effects and also carry out 3D numerical simulations.

Acknowledgments

This research was partially supported by Ministerio de Educación y Ciencia under grant MTM2010-16401 with the participation of FEDER, and Consejería de Educación y Ciencia de la Junta de Andalucía, research group FQM-315. The authors wish to thank the reviewers for useful comments and suggestions which have led to improving the presentation of this paper.

References

[1] K. Chełminski, D. Hömberg, D. Kern, On a thermomechanical model of phase transitions in steel, WIAS preprint, 1125, Berlin, 2007.
[2] J.M. Díaz Moreno, C. García Vázquez, M.T. González Montesinos, F. Ortegón Gallego, Un modelo para la descripción de las transiciones de fases en una barra de acero, Actas XX Congreso de Ecuaciones Diferenciales y Aplicaciones/X Congreso de Matemática Aplicada. Sevilla, 24–28 september 2007.
[3] J.M. Díaz Moreno, C. García Vázquez, M.T. González Montesinos, F. Ortegón Gallego, Numerical simulation of a induction–conduction model arising in steel hardening model arising in steel hardening, in: Lecture Notes in Engineering and Computer Science, World Congress on Engineering 2009, vol. II, 2009, pp. 1251–1255.
[4] J. Fuhrmann, D. Hömberg, M. Uhle, Numerical simulation of induction hardening of steel, COMPEL 18 (3) (1999) 482–493.
[5] D. Hömberg, A mathematical model for induction hardening including mechanical effects, Nonlinear Anal. RWA 5 (2004) 55–90.
[6] A. Bermúdez, J. Bullón, F. Pena, P. Salgado, A numerical method for transient simulation of metallurgical compound electrodes, Finite Elem. Anal. Des. 39 (2003) 283–299.
[7] A. Bermúdez, D. Gómez, M.C. Muñiz, P. Salgado, Transient numerical simulation of a thermoelectrical problem in cylindrical induction heating furnaces, Adv. Comput. Math. 26 (2007) 39–62.
[8] F.J. Pena Brage, Contribución al modelado matemático de algunos problemas en la metalurgia del silicio, Ph.D. Thesis, Universidade de Santiago de Compostela, 2003.
[9] H.M. Yin, Regularity of weak solution to Maxwell's equations and applications to microwave heating, J. Differential Equations 200 (2004) 137–161.
[10] S. Clain, R. Touzani, A two-dimensional stationary induction heating problem, Math. Methods Appl. Sci. 20 (1997) 759–766.
[11] F. Hecht, O. Pironneau, A. Le Hyaric, K. Ohtsuda, Freefem++, http://www.freefem.org/ff++.